

Wijesekara, KKDA, Sadique, M, Carnacina, I, Fielding, A and Bojczuk, GC

**Mechanical and durability analysis of geopolymer concrete made with recycled silicate activator for low carbon breakwaters**

<https://researchonline.ljmu.ac.uk/id/eprint/26531/>

#### Article

**Citation** (please note it is advisable to refer to the publisher's version if you intend to cite from this work)

**Wijesekara, KKDA, Sadique, M, Carnacina, I, Fielding, A and Bojczuk, GC (2025) Mechanical and durability analysis of geopolymer concrete made with recycled silicate activator for low carbon breakwaters. Cleaner Waste Svstems. ISSN 2772-9125**

LJMU has developed [LJMU Research Online](#) for users to access the research output of the University more effectively. Copyright © and Moral Rights for the papers on this site are retained by the individual authors and/or other copyright owners. Users may download and/or print one copy of any article(s) in LJMU Research Online to facilitate their private study or for non-commercial research. You may not engage in further distribution of the material or use it for any profit-making activities or any commercial gain.

The version presented here may differ from the published version or from the version of the record. Please see the repository URL above for details on accessing the published version and note that access may require a subscription.

For more information please contact [researchonline@ljmu.ac.uk](mailto:researchonline@ljmu.ac.uk)



# Mechanical and durability analysis of geopolymer concrete made with recycled silicate activator for low carbon breakwaters

K.K.D.A. Wijesekara<sup>a</sup>, Monower Sadique<sup>a,\*</sup> , Iacopo Carnacina<sup>a</sup>, Alistair Fielding<sup>b</sup> , Gabriela Chronowska Bojczuk<sup>b</sup>

<sup>a</sup> Built Environment and Sustainable Technologies (BEST) Research Institute, School of Civil Engineering and Built Environment, Liverpool John Moores University, Byrom Street, Liverpool L3 3AF, UK

<sup>b</sup> School of Pharmacy and Biomolecular Sciences, Liverpool John Moores University, Byrom Street, Liverpool L3 3AF, UK

## ARTICLE INFO

### Keywords:

Breakwater  
Geopolymer  
Recycled aggregate  
Recycled sodium silicate  
Slake test  
Compressive strength  
Durability

## ABSTRACT

This study investigates the feasibility of using recycled sodium silicate (RSiA) extracted from waste glasses as an alternative to commercial sodium silicate (CSiA) in the production of alkali-activated geopolymer concrete for breakwater applications. The influence of RSiA on the chemical characteristics, mechanical performance, and environmental impact of geopolymer mortars and concrete was evaluated. Elemental composition and FTIR analyses were conducted to characterise the silicate activators, revealing comparable chemical profiles with a notable difference in the SiO<sub>2</sub>/Na<sub>2</sub>O molar ratio (Ms: CSiA = 2.81; RSiA = 1.53). Mortar mixes with varying fly ash (FA) and ground granulated blast furnace slag (GGBS) ratios (e.g., FA:GGBS = 40:60, 80:20) and different Na<sub>2</sub>SiO<sub>3</sub>:NaOH ratios (1:2, 1:1, and 2:1) were tested for compressive strength under various curing regimes, including air, water, and partial hot water curing. Microstructural analysis via SEM and XRD confirmed the formation of dense geopolymer gels and crystalline phases. CO<sub>2</sub> emissions and cost analysis indicated that a 2:1 Na<sub>2</sub>SiO<sub>3</sub>:NaOH ratio minimised both environmental and economic impact. The optimised mix (C40–2111) achieved a compressive strength of ~47 MPa under partial hot water curing, ~35 MPa under air curing and ~33 MPa under water curing after 28 days. Compared to conventional concrete used in coastal defence structures, the RSiA-based geopolymer blocks met or exceeded performance standards in terms of compressive strength, suggesting their suitability as sustainable alternatives to traditional breakwater materials.

## 1. Introduction

Breakwaters are temporary and effective for coastal protection, mitigating the risk of flooding and coastal erosion. The use of detached breakwaters was relatively uncommon in the UK as of early 1998, when only six offshore breakwater initiatives were built in the UK (King et al., 2000). In the coming decades, the littoral areas are predicted to experience problems such as higher design waves, unexpected overtopping, and coastal flooding due to structural damage and flood risks (Muis et al., 2020). Using mass concrete with different shapes for dissipating waves to prevent erosion and landslides is an established practice worldwide. The Environment Agency's national strategy for Flood and Coastal Erosion Risk Management (FCERM) states that coastal defence investments need to provide additional benefits such as creating new habitats, providing amenity value, and capturing carbon. In 2022–2023, the Newlyn Coastal Research and Development Project built 88

eco-blocks around an existing rock armour breakwater in west Cornwall.

Coastal projects that need over-the-water labour, like breakwater construction, are typically more expensive than those that use land-based methods. This is because working over water presents challenges as well as greater mobilising costs when utilising specialised floating equipment. Material type and source are key influences on the cost of the breakwater (Crossman et al., 2003). Unit costs for two offshore breakwater projects ranged from £ 1750 to £ 3304 per metre, according to the Environment Agency Unit Cost Database (2007 edition) (Environment Agency, 2007). The Rock Manual (CIRIA, 2007) outlines various repair and upgrading requirements for breakwaters, including simple maintenance, heavy work, preventative rehabilitation, and full-length replacement. These requirements vary depending on the structure's risk of deterioration, damage, or performance and may require significant dismantling work. The materials in breakwaters might be prone to performance degradation since the seawater can

\* Corresponding author.

E-mail address: [m.m.sadique@ljmu.ac.uk](mailto:m.m.sadique@ljmu.ac.uk) (M. Sadique).

<https://doi.org/10.1016/j.clwas.2025.100322>

Received 12 March 2025; Received in revised form 16 May 2025; Accepted 30 May 2025

Available online 4 June 2025

2772-9125/© 2025 The Authors. Published by Elsevier Ltd. This is an open access article under the CC BY-NC-ND license (<http://creativecommons.org/licenses/by-nc-nd/4.0/>).

induce chemical erosion. Therefore, these materials need to be in compliance with necessary durability standards, assuring the interior materials will not compromise the structural integrity. Concrete exposed to the marine environment is prone to performance degradation under chemical erosion in addition to physical erosion. Therefore, chloride ion permeability affects its service life. Given the high costs and long-term durability challenges associated with traditional materials in breakwater construction, exploring alternative binders such as geopolymer concrete offers a promising route for sustainable coastal infrastructure (Provis & Van Deventer, 2013; Habert et al., 2011).

Geopolymer concrete, an innovative and sustainable alternative to traditional Portland cement-based concrete, has garnered increasing attention due to its potential for reduced carbon emissions and enhanced durability (Singh et al., 2015; Hamed et al., 2025; Provis and Van Deventer, 2013). Life Cycle Impact Assessment (LCIA) by Imtiaz et al. (2021) has shown that global warming potential is reduced by up to 53.7 % by using geopolymer concrete as an alternative to OPC concrete. Geopolymers are a class of inorganic three-dimensional polymers formed by a chemical reaction between an aluminosilicate powder and an alkali solution to raise the pH and dissolve alkali cations in the powder (Davidovits, 2020). These materials are a subclass of alkali-activated materials (AAM) and are reported to possess strong adhesion on a variety of surfaces, low permeability, high mechanical strength similar to OPC concrete when produced with fine and coarse aggregates, and stability against thermal and chemical attack. Emerging research has demonstrated the ability of geopolymers to outperform conventional concrete in extreme environmental conditions, particularly through the incorporation of recycled materials (Shaikh and Haque, 2019; Zhang et al., 2022). Geopolymer concrete has shown superior resistance to chloride penetration and sulfate attack, making it particularly suitable for marine infrastructure (Ostovari et al., 2020; Nath and Sarker, 2017).

Using industrial by-products rich in aluminosilicate sources, such as fly ash (FA), ground granulated blast-furnace slag (GGBS), metakaolin, and similar minerals, as precursors in geopolymer concrete helps reduce waste and conserve natural resources. FA and GGBS as by-products from the coal combustion process in electricity generation plants and pig iron making, respectively, are significant supplies of aluminosilicate precursors for AAM systems. Research indicates that optimized FA-GGBS geopolymer blends can enhance early compressive strength development and long-term durability, crucial for breakwater structures (Vinai et al., 2020; Matsumoto et al., 2021). GGBS is commonly used with Class F fly ash to increase the reactivity of the low-calcium fly ash alkaline binders (Duxson and Provis, 2008). Sodium hydroxide (NaOH), sodium silicate ( $\text{Na}_2\text{SiO}_3$ ), potassium hydroxide (KOH), and potassium silicate ( $\text{K}_2\text{SiO}_3$ ) are the most commonly used activators, either separately or in combination, depending on the needs for the raw materials (precursor) and mix design (Palomo et al., 1999). During the polymerization process, these solutions extract the silicon and aluminum atoms from the source materials to form polymeric silicon-oxygen-aluminum linkages. Research has shown that, despite KOH's higher alkaline nature, NaOH is more effective than KOH at releasing silica and alumina monomers (Davidovits, 1994). In comparison to the case of alkaline hydroxide alone, the polymerization process accelerates when soluble silicates linked to Na or K are present (Palomo et al., 1999).

The conventional manufacturing methods of sodium silicate incur high costs, energy demands, and environmental concerns, including greenhouse gas emissions (Fioletto et al., 2006). Recent studies have explored alternative activators derived from industrial waste, including glass waste-derived sodium silicate, to reduce energy consumption while maintaining mechanical performance (Rodriguez et al., 2013; Puertas et al., 2014). First the solid glass is produced by heating sodium carbonate and natural quartz sand at high temperatures (1400–1500°C) in a specialized furnace and this process involved 403–540 kg/ton of  $\text{CO}_2$  emissions and consumes 420–1250 MJ/ton of energy (European Commission, 2007). Glass is then dissolved in water, filtered, and

evaporated to achieve the desired solution density (Fioletto et al., 2006). Therefore, the synthesis of sodium silicate poses a substantial threat to the sustainability of the geopolymer binder industry. Several research studies have shown that comparable mechanical properties of that of commercial silicates could be achieved by using alternative silicate-based activators such as green olivine nano-silica (Gao et al., 2017), chemically modified nano-silica (Rodriguez et al., 2013), modified silica fume (Zivica et al., 2006), silica fume/rice husk ash with NaOH (Bernal et al., 2012) and industrial glass waste dissolved in NaOH/ $\text{Na}_2\text{CO}_3$  solution (Puertas et al., 2014). Glass waste (GW) makes up 1 % and 5 % of worldwide waste creation for low- and high-income groups, respectively (World Bank Group, What a Waste 2.0, 2018) where soda-lime-silica glass accounts for approximately 90 % of the total amount of glasses produced (Butler et al., 2011). Although they can be used to produce new glass, contamination, colour, and composition reduce the reusable quantities of glass. The UK has set up a recycling target of 60 % for glass waste and achieved it in recent years (Federação dos vidros de embalagem da Europa, 2014). The use of waste glass in alkali-activated systems has been shown to enhance microstructural properties and improve sulphate resistance, making it a viable alternative for sustainable breakwater construction (Dadsetan et al., 2022; Rashidian-Dezfouli et al., 2018). The waste glass cullet, which contains 70–75 % amorphous silica, appears to be an intriguing choice among all materials rich in silica to improve the ecological side of geopolymers. While raw GW was successfully added to the precursor powder, it was shown to significantly impair the mechanical characteristics of geopolymer binders, especially when added in amounts greater than 25 % (Dadsetan et al., 2021(a); Dadsetan et al., 2021(b)). A number of research projects have looked at the feasibility of generating sodium silicate solutions that are easy to use from GW, aiming to minimise the amounts of commercial sodium silicate and optimize the use of GW as precursor and hardener while achieving structural mechanical strengths (Dadsetan et al., 2022). These solutions are intended to be utilised as a liquid hardener in structural geopolymer binders that are made using the least amounts of precursors derived from GW. The total/partial replacement of the usual sodium silicate precursor with waste glass-derived silicate has resulted in satisfactory compressive strength in the alkali-activated mixtures with NaOH (Rashidian-Dezfouli et al., 2018; Vinai and Soutsos, 2019). There are different methods used to extract sodium silicate from waste glass, such as hydrothermal methods, which involve heating glass in alkaline solutions, and thermochemical (fusion) methods, which involve glass and NaOH mixing. Aluminosilicate precursors and alkali silicates, also referred to as hardeners, are typically the source of silica in geopolymers. Several variables, including particle size, the alkalinity of the surrounding environment, and polymorph or amorphous structure, affect the depolymerization and dissolution of silica in the precursor.

Construction and demolition waste (CDW) generates a huge number of debris globally and has become an unavoidable problem. Fisher and Werge (2009) report that CDW represents 31 % of overall waste, where ~850 million tonnes of CDW are generated in the European Union (EU) annually. The recycling of CDW as aggregate to produce new concrete has, therefore, become a common practice to reduce the problem of waste, which preserves natural aggregate (NA) resources. There are two types of RAs derived from CDW: (1) Mixed Recycled Aggregates (MRAs) – heterogeneous, produced in higher quantities, and can hardly be used in structural concrete and (2) Recycled Concrete Aggregates (RCA) – lower heterogeneity content, anticipated to be utilized for structural concrete production. MRAs and RCAs, respectively, reported to yield average compressive strength values of 35 MPa and 45 MPa (Piccinali et al., 2022). Recent advancements in RCA utilization for marine geopolymer concrete applications have shown that careful mix design can yield durable and high-compressive-strength materials suitable for harsh environments (Piccinali et al., 2022; Gholampour et al., 2023). The curing process, a critical phase in concrete development, significantly shapes the final characteristics of geopolymer concrete

(Akduman et al., 2024; Gaurav et al., 2024). Optimization of curing regimes has been found to enhance the durability of geopolymer concrete, with room-temperature curing proving effective for large-scale applications such as breakwaters (Shoaei et al., 2024; Kanagaraj et al., 2024).

Despite the growing interest in geopolymer concrete for marine applications, long-term durability under real-world exposure conditions remains a critical research area. Studies have emphasized the need for extended service life assessments, particularly in aggressive marine environments, where factors such as chloride ingress can significantly degrade material performance (Zhang et al., 2020; Gitto et al., 2023). The long-term performance of geopolymer-based breakwaters is strongly influenced by fluctuating temperature regimes and variations in salinity. Thermal cycling, typical in coastal zones, can induce micro-cracking due to differential expansion between the geopolymer matrix and aggregates; however, geopolymer binders exhibit lower coefficients of thermal expansion ( $8\text{--}10 \times 10^{-6} \text{ }^\circ\text{C}^{-1}$ ) than OPC concretes ( $10\text{--}15 \times 10^{-6} \text{ }^\circ\text{C}^{-1}$ ), which mitigates crack propagation under diurnal temperature swings (Temuujin et al., 2010). Moreover, repeated heating and cooling enhances microstructural densification via further geopolymerization of residual aluminosilicate phases, thereby improving resistance to subsequent mechanical loads. Salinity gradients pose another challenge: chloride and sulfate ions in seawater can attack conventional OPC matrices by promoting corrosion and sulfate-induced expansion. Incorporating Life Cycle Assessment (LCA) methodologies tailored for marine environments reveals that while geopolymer concretes offer lower embodied carbon compared to Portland cement systems, durability performance directly affects their long-term environmental and economic efficiency (Habert et al., 2011; Law et al., 2015). Therefore, integrating long-term exposure testing and durability modelling is essential for validating the use of recycled-activator-based geopolymer concrete in breakwater construction.

Unlike conventional geopolymer systems, this study introduces the use of a recycled silicate activator (RSiA), derived from cathode ray tubes (CRT) and domestic waste glass, as a sustainable alternative to commercial silicate solutions. The innovative contribution lies in integrating this recycled activator into a geopolymer concrete mix specifically designed for breakwater and other non-structural marine applications. The project aims to develop an industrial-scale, cement-free concrete incorporating recycled aggregates (RA) and RSiA, with a focus on long-term durability and reduced embodied carbon footprint. Key objectives include: (a) evaluating optimum mix ratios of GGBS:FA and  $\text{Na}_2\text{SiO}_3$ :NaOH in relation to compressive strength, cost, and carbon footprint; (b) determining the most effective curing conditions to meet performance requirements; and (c) assessing durability through marine-relevant tests such as slake durability and chloride migration. This multi-criteria optimization approach offers a more holistic validation framework than prior research and represents a novel step toward circular, resilient, and environmentally conscious coastal infrastructure.

## 2. Materials and methods

### 2.1. Materials

Ground granulated blast furnace slag (GGBS), pulverised fly ash, (PFA), were used as alumina and silica- and silica-containing solid precursor sources, respectively, to develop a non-Portland mix. For the control mix, Ordinary Portland Cement (OPC). Cement is OPC type CEM II, class of compressive strength 32.5 N used (which was the target strength of concrete produced) as per BS EN 197-1:2011. The activators used represent the alkaline source that increases the pH of the chemical reaction and eases the dissolution. For this research, the liquid activators Sodium hydroxide (NaOH), and Sodium silicate ( $\text{Na}_2\text{SiO}_3$ ), were used. Sodium hydroxide solution (4 M) from Fisher Scientific and commercial sodium silicate (CSiA), Technical, Solution, d= 1.5 from Fisher Chemical, was used to prepare the alkali activator. A recycled silicate activator

(RSiA) was extracted from crushed waste glass from cathode ray tubes (CRT) and domestic waste glass by a local waste management organisation. 1 ton of glass (<1 mm) crushed at  $110^\circ\text{C}/15 \text{ kW}$  yields 2.5 tons of liquid recycled silicate activator. Irrespective of the volume of raw meal, the extraction process takes around 4–5 h.

Natural aggregates (NA), include coarse aggregates with 10 mm and 20 mm aggregates and fine aggregates (commercial sand) with a size under  $600 \text{ }\mu\text{m}$  that accords with the British Standard BS EN 12620:2002 +A1:2008. The quantity of 10 mm and 20 mm was adjusted to get similar particle size distribution to that of recycled aggregates.

Recycled aggregates (RA) were supplied by a local waste management organization that processes CDW. This consists of a combination of different materials (ceramic, plastic, metal, clay, glass, concrete or stones), densities, shapes, roughness, and porosities. The PSD was determined by dry sieving according to the BS ISO 20977:2018. Fig. 1 shows the images of aggregates used to interpret their sizes and the particle size distribution of RA. Equal mixtures of 10 mm and 20 mm of natural coarse aggregates were used to resemble the sizes of RA.

### 2.2. Testing procedure

#### 2.2.1. Characterisation of RSiA

The elemental composition (by EDX) and chemistry (by FTIR) of CSiA and RSiA were analysed to evaluate the chemical characteristics of the recycled silicate in comparison to its commercial counterpart, as these variations may influence the resultant properties of geopolymer concrete. The EDX containing Oxford Inca x-act detector with probe current 45 nA and counting time 100 sec and FEI SEM model Inspect S with accelerating voltage 20 kV was used for the elemental analysis. Fourier transform infrared (FT-IR) spectra recorded on an Agilent Cary 630 FTIR spectrometer, using a Diamond-Attenuated total reflectance (ATR) sampling module in transmission. Spectra were recorded using 2 scans at a resolution of  $2 \text{ cm}^{-1}$ .

#### 2.2.2. Mechanical strength of mortars - optimisation of mix design and curing condition

**2.2.2.1. Mix design.** The mix design procedure was optimized to study the effects of varying the ratios of fly ash (FA) to GGBS and the  $\text{Na}_2\text{SiO}_3$  to NaOH solution ratio. These parameters were selected based on their influence on the mechanical properties and durability of the geopolymer concrete. The design followed guidelines specified in BS EN 196-1 (British Standard Institution, 2016) for mortar mix preparation. The mix ratios were carefully adjusted to maintain a binder-to-fine aggregate ratio of 1:1, a liquid-to-binder ratio of 0.4, and a total aggregate-to-binder ratio of 3:1 to produce mortars ( $40 \text{ mm} \times 40 \text{ mm} \times 160 \text{ mm}$ ) with a density of  $2404 \text{ kgm}^{-3}$ . This specimen size was selected in accordance with the standard to ensure reliable and comparable compressive strength testing, as it allows for accurate measurement of compressive strength, facilitating the evaluation of mechanical performance under standardised conditions. The following mix designs are as in Table 1 were tested:

The mix ratios were chosen to assess the effects of the different proportions of fly ash and GGBS, as well as variations in alkali solution concentrations. The 1:1, 1:2, and 2:1  $\text{Na}_2\text{SiO}_3$ :NaOH ratios were tested to observe the impact of different levels of alkalinity on the geopolymerization process. The mix ID C40-2111 represents that the mix consists of FA:GGBS at 40:60 and  $\text{Na}_2\text{SiO}_3$ :NaOH at 2:1 and binder: fine aggregate 1:1.

**2.2.2.2. Curing conditions.** Curing is a crucial factor in the development of geopolymer concrete compressive strength. In this study, the impact of different curing conditions was assessed:



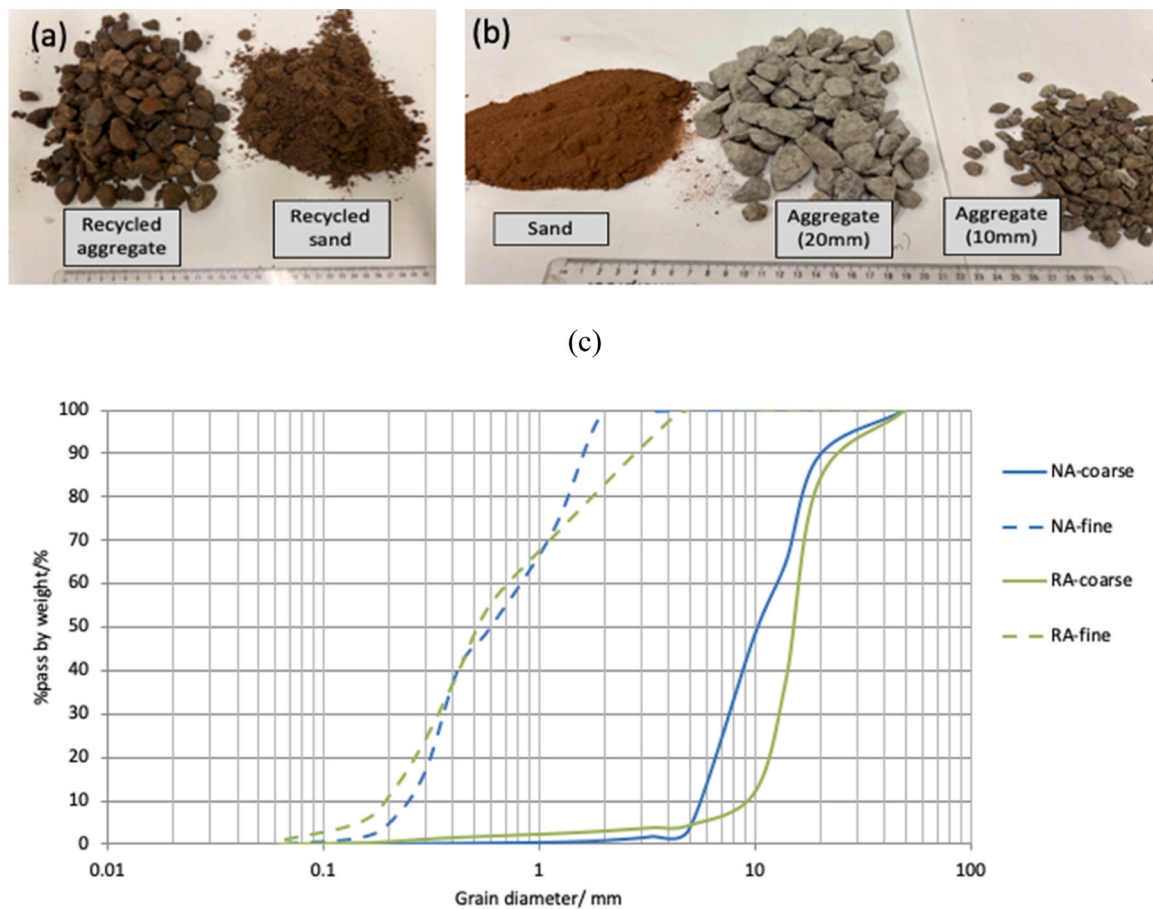


Fig. 1. Images of (a) RA (b) NA. Scale in mm, (c) particle size distribution of commercial and recycled coarse/fine aggregates.

Table 1

Mix design of blocks prepared for compressive strength comparison.

Mix ID	FA: GGBS	Na <sub>2</sub> SiO <sub>3</sub> : NaOH	Binder: Fine Aggregate
C40–1111	40:60	1:1	1:1
C80–1111	80:20		
C90–1111	90:10		
C40–1211	40:60	1:2	
C80–1211	80:20		
C90–1211	90:10		
C80–2111	80:20	2:1	
C40–2111	40:60		

1. Air Curing (AC): Specimens were kept at room temperature (20°C) for the curing period.
2. Room Temperature Water Curing (RTWC): Specimens were immersed in water at room temperature.
3. Partial Hot-Water Curing (PHWC): Mortars were initially cured in water at 50°C for 3 days, followed by air curing for the remainder of the curing period.

Mortars made of C40–2111 and C80–2111 mix designs using commercial silicate were used to study their effectiveness in promoting the geopolymerization reaction and strengthening the geopolymer concrete. The effect of curing regime (AC, RTWC and PHWC) on compressive strength was then tested using RSiA for the mortars with mix designs C40–1111, C80–1111 and C40–2111.

By adjusting these mix ratios and curing conditions, the study aimed to optimize the geopolymer mix for improved mechanical strength, durability, and sustainability, as well as to evaluate the potential of using RSiA as a substitute for conventional silicate aggregates.

### 2.2.3. Mechanical strength of concrete blocks – comparative study

To evaluate the mechanical strength properties of concrete incorporating RSiA, concrete cubes measuring 100 mm × 100 mm × 100 mm were produced following the C40–2111 mix design. The mix design adhered to the British Standard BS EN 206:2013 for concrete mix proportions and BS EN 12390–3:2019 for compressive strength testing. These samples were subjected to different curing conditions (AC, RTWC, and PHWC) to assess their impact on mechanical performance.

The suitability of RSiA as a substitute for conventional silicate activators was assessed by comparing different mix designs using various combinations of normal and recycled aggregates, as well as commercial and recycled silicate activators. All mixes were made using a total aggregate: binder ratio of 3:1, a liquid: binder ratio of 0.4, and a binder: fine aggregate ratio of 1:1. C40–2111 design comprised FA:GGBS = 40:60, Na<sub>2</sub>SiO<sub>3</sub>: NaOH = 2:1 and binder: fine aggregate = 1:1 as mentioned in Table 1. The following mix designs were considered:

1. Normal concrete with NA (NC -NA)
2. Normal concrete with RA (NC -RA)
3. Geopolymer mix (C40–2111) using commercial silicate and NA (GEO - CSiA -NA)
4. Geopolymer mix (C40–2111) using RSiA and NA (GEO - RSiA - NA)
5. Geopolymer mix (C40–2111) using RSiA and RA (GEO-RSiA - RA)

### 2.2.4. Embodied carbon and cost comparison

The selection of the optimum mix design was based on a comprehensive analysis of mechanical strength in relation to cost-effectiveness and environmental impact, particularly the embodied carbon footprint of the material mix. The evaluation process involved comparing the cost and carbon footprint of different material compositions to determine the

most sustainable and economical mix for use in geopolymer concrete blocks.

**2.2.4.1. Material cost analysis.** The cost analysis was conducted considering the prices of raw materials, including FA, GGBS,  $\text{Na}_2\text{SiO}_3$ , NaOH, NA, and RA. The cost variation between commercial silicate activators (CSiA) and recycled silicate activators (RSiA) was specifically analysed to determine the economic benefits of using RSiA in geopolymer concrete production. The cost per unit volume of each mix was calculated to facilitate a direct comparison of material expenses.

**2.2.4.2. Embodied carbon assessment.** The embodied carbon footprint of each material mix was assessed using standardized carbon accounting methodologies as per the ISO 14067:2018 standard for carbon footprint quantification. The greenhouse gas emissions associated with each constituent material were analysed, including emissions from raw material extraction, processing, transportation, and manufacturing. A global average value of 0.475 kg  $\text{CO}_2\text{e}/\text{kWh}$  of greenhouse gas emission intensity for electricity generation ( $I_{\text{GHG}}$ ) was applied for embodied carbon calculations considering  $I_{\text{GHG}}$  in EU-27 conservatively (0.265 kg  $\text{CO}_2\text{e}/\text{kWh}$ ), China (0.531 kg  $\text{CO}_2\text{e}/\text{kWh}$ ) and USA (0.376 kg  $\text{CO}_2\text{e}/\text{kWh}$ ) estimations (European Environment Agency, 2023; EIA, U.S. Energy, 2023; EMBER China, 2023). The embodied carbon footprint of each material mix was then computed based on the cumulative emissions of individual components.

## 2.2.5. Durability characteristics of blocks

**2.2.5.1. Density and surface porosity of hardened concrete.** To assess the density and surface porosity of the hardened concrete, standardized testing procedures were followed in accordance with ASTM C642–21 (Standard Test Method for Density, Absorption, and Voids in Hardened Concrete). The specimens (volume  $>60$  cm and surface area to volume ratio between  $0.08 \text{ mm}^{-1}$  and  $0.20 \text{ mm}^{-1}$ ) were dried at  $(70 \pm 5)^\circ\text{C}$  until a constant mass ( $m_d$ ) and evacuated gradually to  $(2.0 \pm 0.7) \text{ kPa}$  ( $(15 \pm 5) \text{ mmHg}$ ) in an evacuation vessel. This pressure was maintained for  $(2 \pm 0.2) \text{ h}$  to eliminate the air contained in the open pores of the specimens and demineralized water was slowly introduced at  $(20 \pm 5)^\circ\text{C}$  into the vessel (the rate at which the water rises shall be such that the specimens are completely immersed not less than 15 min). When all the specimens were immersed, the vessel was returned to atmospheric pressure, and the specimens were left underwater for another  $(24 \pm 2) \text{ h}$  at atmospheric pressure. Then, each specimen was weighed under water ( $m_b$ ), and the mass was recorded in water and weighed again after quickly wiping the specimen ( $m_s$ ) with a dampened cloth, and the mass of the specimen saturated with water was determined. The volume of the open pores ( $V_o$ ) in millilitres and the apparent volume ( $V_b$ ) (in millilitres) are calculated by,

$$V_o = \frac{ms - md}{\rho_{rh}} \times 1000 \quad (\text{i})$$

$$V_b = \frac{ms - mh}{\rho_{rh}} \times 1000 \quad (\text{ii})$$

The value of the density of water  $\rho_{rh}$  at  $20^\circ\text{C}$  is  $998 \text{ kgm}^{-3}$  apparent density.

The apparent density (in  $\text{kgm}^{-3}$ ) is expressed by the ratio of the mass of the dry specimen and its apparent volume, by the equation:

$$\rho_b = \frac{md}{ms - mh} \times \rho_{rh} \quad (\text{iii})$$

The open porosity is expressed by the ratio (as a percentage) of the volume of open pores and the apparent volume of the specimen, by the equation:

$$Po = \frac{ms - md}{ms - mh} \times 100 \quad (\text{iv})$$

These calculations provide insight into the pore structure and density characteristics of the hardened concrete, crucial for evaluating its durability and resistance to environmental influences.

**2.2.5.2. Slake durability test.** The slake durability test was carried out in accordance with ASTM D4644–16 (ASTM International, 2016) to evaluate the resistance of hardened concrete specimens to weathering and erosion when exposed to wet-dry cycles. Ten specimens, each weighing between 40 and 60 g (with the total initial mass recorded), were placed inside a wire mesh drum as shown in Fig. 2, which is partially submerged in a trough filled with deionized (DI) water. The drum was then rotated at 20 rpm for 10 min, and the total mass of the specimen retained in the drum was measured after oven drying. This was repeated for 2 cycles. Based on the recorded total masses of test specimens kept in the drum for each cycle, the slake durability index is computed.

Slake durability index ( $I_d$ ) was calculated as below.

After cycle 1:

$$Id1 = \frac{m_{C1}}{m_i} \times 100 \quad (\text{v})$$

After cycle 2:

$$Id2 = \frac{m_{C2}}{m_i} \times 100 \quad (\text{vi})$$

Where,  $m_i$  – Initial mass of the specimens  $m_{C1}$  – Mass of the specimens after cycle 1  $m_{C2}$  – Mass of the specimens after cycle 2

This test method is particularly useful for assessing the durability of geopolymer concrete, resulting in a measure of the ability of the concrete to withstand repeated wetting and drying cycles.

**2.2.5.3. Chloride migration test.** The chloride migration test was conducted following BS EN 12390–18:2021 (British Standards Institution, 2021), which specifies the procedure for assessing the chloride migration coefficient in hardened concrete. This test evaluates the resistance of concrete to chloride ingress, which is crucial for determining its durability in aggressive environments, particularly in structures exposed to marine conditions or de-icing salts. The test was carried out at 7, 14, and 28 days of curing age to assess the chloride migration coefficient. Cylindrical test specimens ( $\varnothing 100 \text{ mm}$ ,  $h \sim 50 \text{ mm}$ ) fitted into rubber sleeves were immersed in the catholyte solution, 0.3 N (normality) NaOH, and each migration cell was filled with  $\sim 300 \text{ ml}$  of 5 % NaCl in 0.3 N NaOH. An external potential was applied to facilitate the chloride ions in the catholyte solution to migrate into the specimen. After 168 h (7 days), the specimens were disassembled and dissected as in Fig. 3), and the depth of chloride penetration was determined using silver nitrate.

## 3. Results & discussion

### 3.1. Characterisation of CSiA and RSiA

The chemical and structural properties of the commercial sodium silicate activator (CSiA) and the recycled sodium silicate activator (RSiA) were assessed through elemental analysis and FTIR spectroscopy to evaluate the suitability of RSiA in geopolymer binder systems. Elemental composition and FTIR spectra for CSiA and RSiA are presented in Table 2 and Fig. 4, respectively.

Sodium silicate is a generic appellation that exists in the form of  $\text{Na}_2\text{xSiO}_{2+\text{x}}$  and, therefore, as a series of alkaline silicate compounds (Liu and Ott, 2020). Two characteristics of sodium silicate solutions are typically identified: the  $\text{SiO}_2$  content and the modulus (Ms), which is the molar ratio of  $\text{SiO}_2$  to  $\text{Na}_2\text{O}$  (Nordström et al., 2011). Calculated values





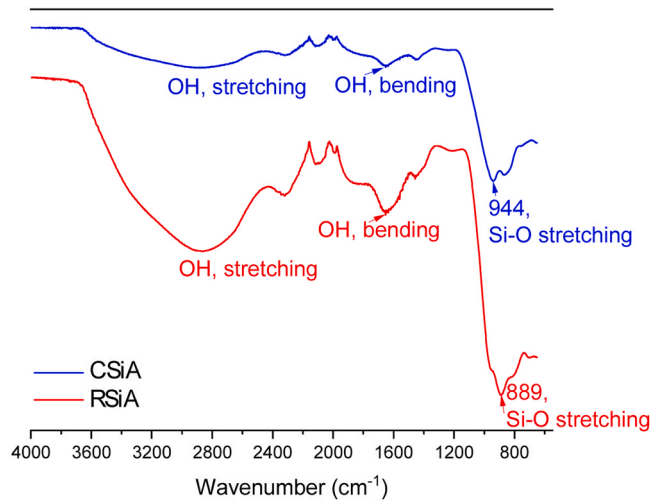
Fig. 2. Experimental setup for the slake durability test.



Fig. 3. Chloride migration test set up for the cylindrical samples and bisected samples.

**Table 2**  
Elemental composition of CSiA and RSiA.

Element	CSiA	RSiA
O	56.2	59.3
Na	16.1	21.0
Si	27.7	19.7



**Fig. 4.** ATR-FTIR transmission spectra of CSiA (blue) and RSiA (red).

for Ms from elemental analysis results of CSiA and RSiA are 2.81 and 1.53, respectively. Reddy et al. (2021) varied Ms from 1.50 to 3.00 for different ratios of  $\text{Na}_2\text{SiO}_3/\text{NaOH}$  (2.0, 2.5 and 3.0) and for various concentrations of NaOH (8 M, 10 M, 12 M, 14 M, 16 M and 18 M) and

resulted that the 16 M NaOH yields high compressive strength when  $\text{SiO}_2/\text{Na}_2\text{O}$  in  $\text{Na}_2\text{SiO}_3$  solution is around 2.00–2.40 and  $\text{Na}_2\text{SiO}_3/\text{NaOH} = 2.5$ .

ATR-FTIR analysis was performed to check if there are any significant differences in CSiA and RSiA as shown in Liu and Ott, 2020. RSiA shows slightly broadening of the peak associated with Si-O stretching at  $889\text{ cm}^{-1}$  compared to that of CSiA at  $944\text{ cm}^{-1}$  (Stuart, 2004), attributed to the amorphous nature of the RSiA (James et al., 2010). Additional bands at  $\sim 1640\text{ cm}^{-1}$  and  $3000\text{ cm}^{-1}$  are assigned to the stretching and bending vibrations of OH, respectively, and high-intensity peaks for RSiA compared to CSiA reflect the presence of high levels of water in RSiA. No significant new bands were observed apart from the greater water content in RSiA, suggesting similar chemistry as in CSiA.

### 3.2. Mix design optimization (GGBS-FA and $\text{Na}_2\text{SiO}_3/\text{NaOH}$ ratio)

#### 3.2.1. Impact on compressive strength

Compression strength values of different mortar mixes after 7-, 14- and 28-days air curing are presented in Fig. 5. C40 mixes that contained FA: GGBS at 40:60 produced higher compressive strength (above 38 MPa) for more than 28 days curing compared to the mixes with FA: GGBS ratio 80:20 and 90:10 (below 25 MPa). Although C80–1111 mix achieved high early age compressive strength (after 7 days curing) it did not gain compressive strength with curing age (after 28 days curing). JTS 154–1–2011 Code for Design and Construction of Breakwater estimated that the average distribution loads of breakwater concrete protective layer (with density  $2300\text{ kgm}^{-3}$ ) are  $24.15\text{ kN/m}^2$  for 5-t accropode blocks and  $12.19\text{ kN/m}^2$  2.8-t square hollow blocks. Conventional breakwater materials, typically OPC-based, are designed to achieve compressive strengths ranging between 20–40 MPa, depending on environmental exposure and design requirements (U.S. Army Corps of Engineers, 2002; ICE Manual of Geotechnical Engineering, 2012).

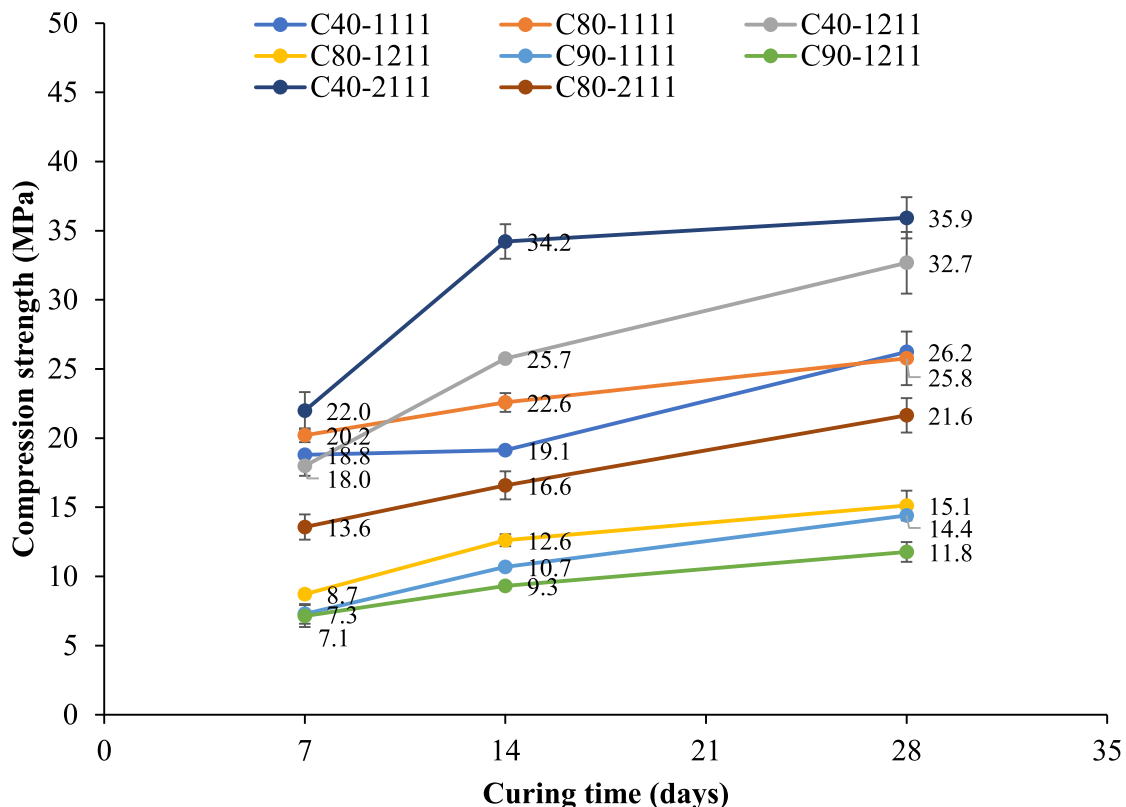


**Fig. 5.** Compression strength of CSiA-based mortars with different mixes cured for 7, 14, and 28 days in air.

Therefore, the C40 mix demonstrates equivalent or superior performance to standard OPC concrete used in breakwaters. Ali et al., 2017 have published guidelines for mix proportioning of fly ash/GGBS based alkali activated concretes using binder mixes with FA:GGBS ratios 100:0, 80:20, 60:40 and 30:70 which resulted compressive strengths 12–20 MPa, 30–40 MPa, 50–60 MPa and 65–75 MPa respectively. These results also confirmed that increasing GGBS content has enhanced the compressive strength (Ali et al., 2017; Dineshkumar et al., 2020).

### 3.2.2. Effect on carbon footprint

CO<sub>2</sub> emissions and price per 100 mm × 100 mm × 100 mm concrete cube with three different Na<sub>2</sub>SiO<sub>3</sub>: NaOH ratios 1:2, 1:1, and 2:1 are presented in Fig. 6. The use of 2:1 of Na<sub>2</sub>SiO<sub>3</sub>: NaOH ratio resulted in the lowest carbon footprint and cost, as NaOH has a significantly high carbon footprint and is the most expensive material in the mix. Therefore, the mix composition C40–2111 was used to produce geo-blocks, considering all three mixes C40–1211, C40–1111, and C40–2111 in their mortars achieved the highest compressive strengths after 28 days of curing (refer Fig. 7). Koushkbaghi et al. (2019) found that when the Na<sub>2</sub>SiO<sub>3</sub>/ NaOH mass ratio increased from 2:1–3:1, it improved the compressive strength while decreasing water by 5.5–10 % and reducing chloride migration. Embodied carbon and cost were considered as crucial factors to decide the silicate-to-alkali ratio of the geo-block.

### 3.2.3. Influence of curing conditions

Mechanical performance of RSiA-based mortars, C40–1111 and C80–1111, cured in air, water, and 3 days of hot water curing, then air curing, is presented in Fig. 7. The best performance of mechanical strength was observed with 3 days hot water cured and then air cured samples, indicating PHWC accelerates compressive strength gain of the mix to almost its maximum strength. Air curing has resulted in better performance compared to water curing in both C40 and C80 mixes. Previous studies have also shown that high-temperature curing increases the compression strength in geopolymer concrete (Yilmaz et al., 2024; Tuyan et al., 2018). C40 mixes with cured in both air and water, complies with grade C25, and can be used for construction in all areas.

Compressive strength gain in RSiA-based mortar samples made with C40–2111 and C80–2111 designs was compared by curing in air and water. The C40 water-cured mix showed the best compressive strength gain, while C80 water-cured and C40 air-cured mortar samples gained similar compressive strength values, as depicted in Fig. 8.

### 3.3. Mechanical strength of RSiA/RA-Based concrete

Since C80 mixes showed adverse effects on compressive strength performance when air-cured, and air curing is the most practical and environment-friendly curing method, C40–2111 mixes were chosen to produce geo-blocks and to assess their durability characteristics. The effect of curing conditions on optimised mix (C40–2111) was explored for the C40-GEO-RSiA- RA mix to explore the behaviour of RSiA in concrete. Fig. 9 presents the mechanical strength results of the concrete cubes C40–2111 made with RSiA cured in air, water, and hot water for 3 days, then in air. PHWC results ~47 MPa, while air curing and water curing results ~35 MPa and ~33 MPa respectively after 28 days. The optimized RSiA/RA-based mix (C40–2111) therefore proves to meet or exceed the mechanical strength demands for coastal defence structures, 20–40 MPa making it a viable candidate for use in breakwater protective layers. Poornima et al. 2021 reported similar compressive strength results where they used blend ratios GGBS 100 %, 75 %, 50 %, and 25 % in FA and resulted from 35 to 48 MPa and 28–45 MPa in water and air curing, respectively, after 28 days.

#### 3.3.1. Microstructure and mineralogy of recycled silicate in geopolymer mix

Microstructure analysis via SEM imaging of C40–21 pastes made of commercial silicate and RSiA are presented in Figs. 10 and 11. Both CSiA and RSiA containing pastes showed a well-cemented surface (shown in yellow arrows in X1000 magnified images) in all curing conditions air, water and partial hot water. This demonstrates the geopolymerization products, C-S-H and A-S-H gels, produced from the aluminosilicate precursors, GGBS and FA. The previous studies have also observed homogeneous geopolymer matrices in SEM images (Yilmaz et al., 2024). All paste mixes exhibited unreacted cenospheres of FA particles along with the dense microstructure. These have also been observed by Aissa et al. (2019), and these particles are reported to enhance the compressive strength with aging, although they do not act as fillers in the matrix (Ryu et al., 2013).

XRD analysis was also carried out on the C40–21 pastes with CSiA and RSiA to investigate the condition of products formed under different curing conditions and the spectra for each composition are shown in Fig. 12. Calcite and mullite components were formed as a result of geopolymerization together with the main quartz component. The peak for calcium silicate hydrate peak is well resolved in water and hot water cured samples compared the air cured ones.

Despite the very high compressive strengths produced in PHWC geopolymer concrete, air curing is a more practical and sustainable curing method for mass-scale GPC production.

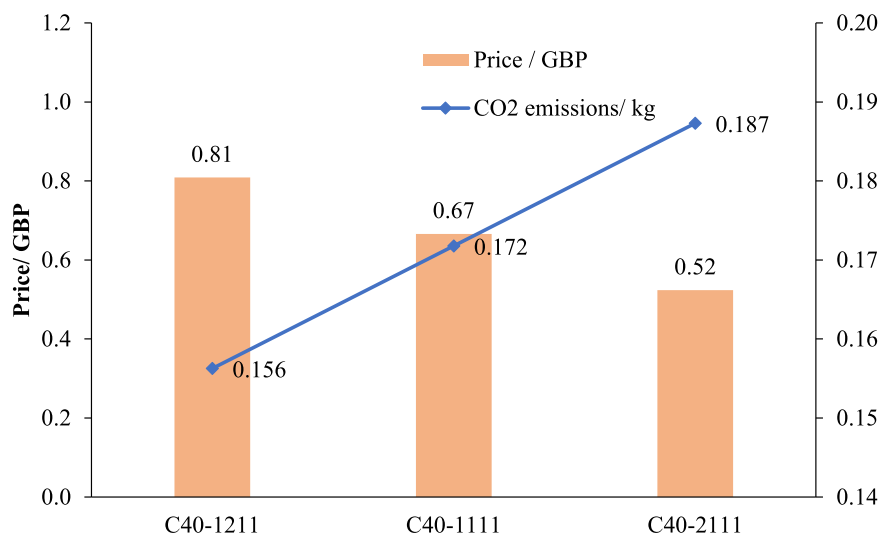


Fig. 6. Price and CO<sub>2</sub> emissions per 100 mm x 100 mm x 100 mm concrete cube with three different Na<sub>2</sub>SiO<sub>3</sub>: NaOH ratios 1:2, 1:1 and 2:1.



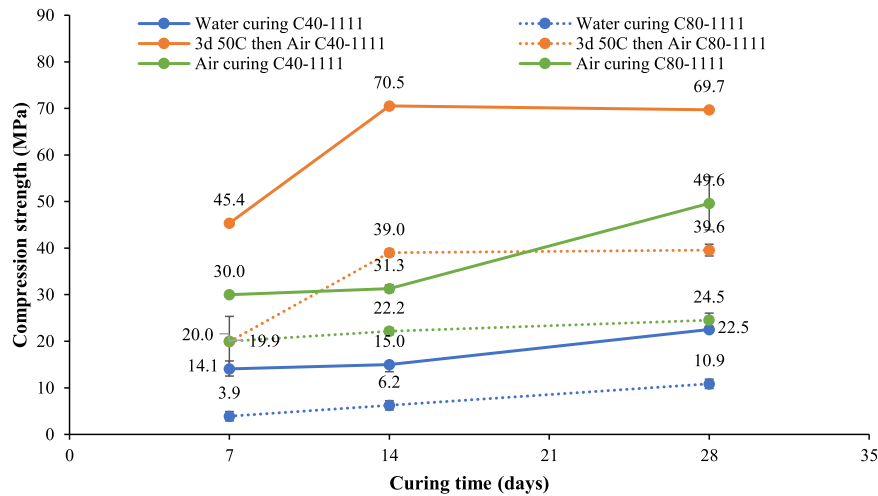


Fig. 7. Compression strength of C40-1111 and C80-1111 mortar blocks cured in water, air and 3 days hot water and then in air.

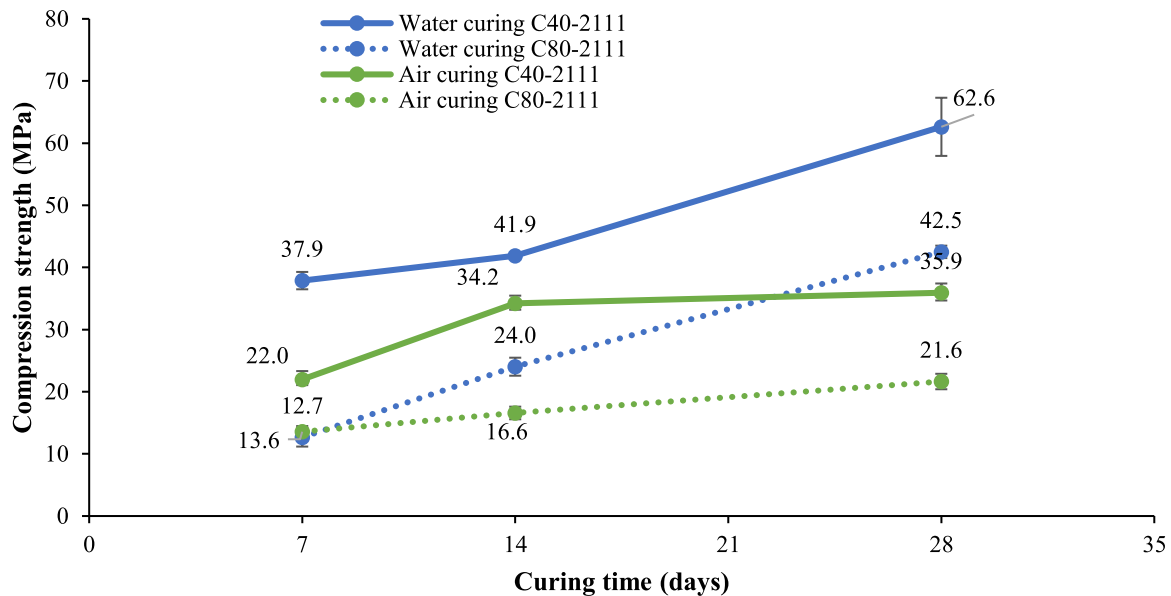


Fig. 8. Compression strength of C40-2111 and C80-2111 mortar blocks (RSiA-based) cured in water and air.

### 3.3.2. Comparison study – performance of RSiA-based geoblocks

Mechanical strength of all mix designs, NC -NA, NC -RA, GEO - CSiA -NA, GEO - RSiA - NA, and GEO-RSiA - RA (Geoblocks produced with mix design C40-2111) are depicted in Fig. 13 to understand the effect of using RA and RSiA in concrete blocks. Replacing NA with RA and replacing CSiA with RSiA have not impacted the compressive strength of the normal concrete respectively after 7, 14, and 28 days.

Nuaklong et al. (2016) used MRAs in the high-calcium fly ash geopolymer concretes and resulted in compressive strengths of 30.6–38.4 MPa after 7 days, which was 76–93 % of that of geopolymer concretes with crushed limestone.

Price and CO<sub>2</sub> emissions by NC-NA, GEO-CSiA-NA, GEO-CSiA-RA and GEO-RSiA-RA per 1 MPa of compressive strength they produced is calculated and compared in Fig. 14. All the geopolymer concrete blocks produce three times less CO<sub>2</sub> emissions per 1 MPa of strength they produce compared to those of normal concrete. Replacing silicate and the aggregate with recycled materials has reduced the price and CO<sub>2</sub> emissions per MPa of compressive strength of geopolymer concrete by 13.8 % and 45.1 %, respectively. Moreover, the use of GEO-RSiA-RA offers a cost-effective alternative to GEO-CSiA-NA, addressing its

economic limitations compared to NC-NA and demonstrating the practicality and adaptability of the recycled mix for breakwater applications.

Imtiaz et al. (2021) carried out a life cycle assessment (LCA) of concrete, geopolymer concrete, and recycled aggregate-based geopolymer concrete and showed that using geopolymer concrete reduces global warming potential by 53.7 % compared to OPC concrete. Using GP concrete reduces acidification potential and photochemical oxidant formation in the impact categories, along with climate change. The presence of alkali activators increases the potential impacts of marine aquatic ecotoxicity, freshwater aquatic ecotoxicity, human toxicity, eutrophication potential, ozone depletion potential, and terrestrial aquatic ecotoxicity potential when using geopolymer concrete (Imtiaz et al., 2021). Therefore, the use of recycled sodium silicate and recycled aggregates geopolymer concrete in the current study reduces all of the above environmental impacts. This eco-efficiency aligns with the increasing emphasis on low-carbon construction in civil infrastructure (ISO 14067:2018; UNEP, 2021) and offers a distinct advantage for large-scale coastal projects, where material volume and environmental exposure are substantial.

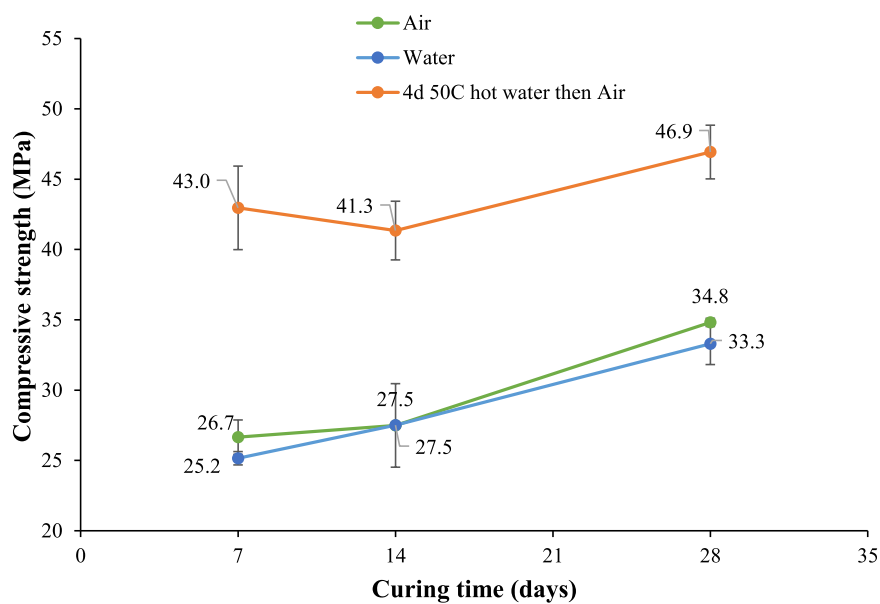


Fig. 9. Compression strength of C40-2111 concrete cubes cured in water, air and 3 days hot water and then in air.

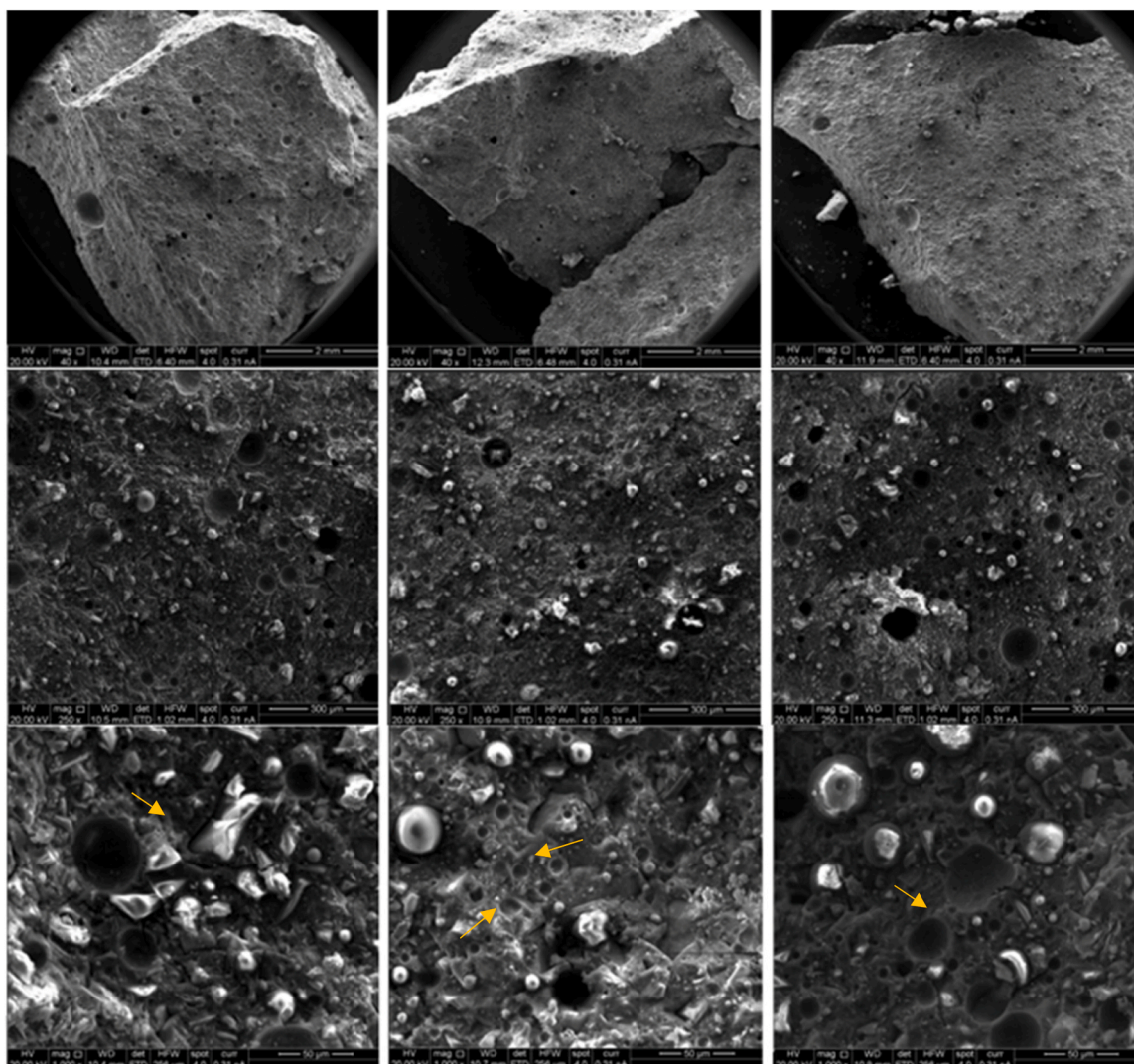


Fig. 10. Microstructure of pastes made of GGBS, FA, commercial silicate and NaOH cured in (left) air, (middle) water, (right) 3d hot water, and then air for 28 days.



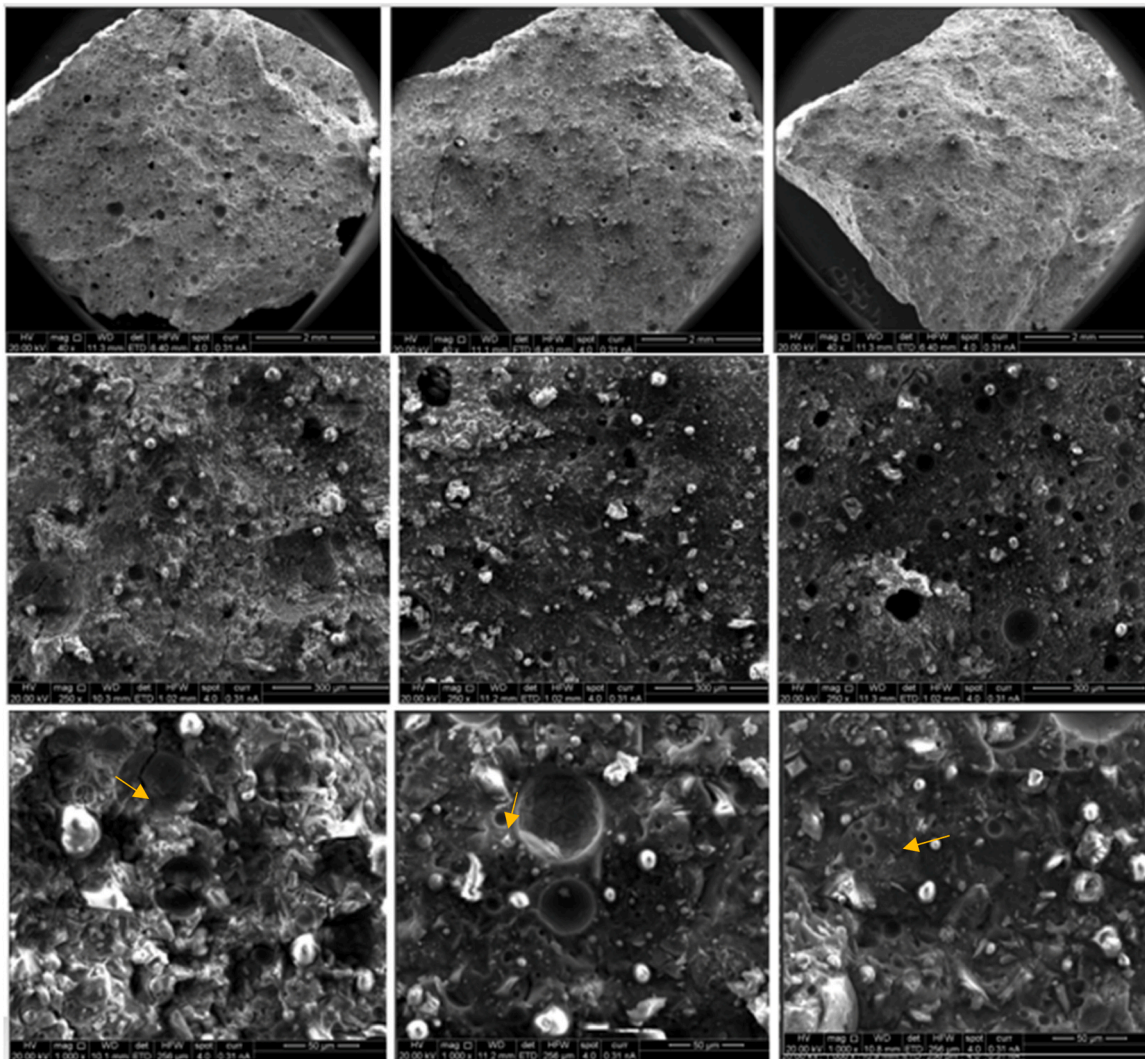


Fig. 11. Microstructure of pastes made of GGBS, FA, RSiA and NaOH cured in (left) air (middle) water (right) 3d hot water and then air.

### 3.4. Durability characteristics of blocks

#### 3.4.1. Density and surface porosity of hardened concrete

Open porosity and apparent density values calculated from triplicate samples of each mix at curing ages of 7, 14, and 28 days are presented in Fig. 15. Geo-blocks made with NA resulted in higher apparent density compared to normal concrete made with cement, while the geo-blocks made with RSiA, and recycled aggregate resulted in comparably lower density. This could be a result of low-density brick pieces present in RA compared to hard natural aggregate. Many studies have reported that the more RAs incorporated, the higher the water absorption by the concrete (Nuaklong et al., 2016; Parthiban and Mohan, 2017; Kathirvel and Kaliyaperumal, 2016), where pore volume and density reflect the water absorption. Lyu et al. (2023) showed that the water absorption rate increased from 14.29 % to 23.4 %, 2.86–20.41 %, and 14.29–102 % when the RA replacement rate is 30 %, 50 %, and 100 %, respectively. They claimed that this is due to increased porosity and the introduction of water channels from RA derived from old mortar and the mechanical damage caused by the crushing process of waste concrete.

#### 3.4.2. Slake durability

Slake durability index ( $I_d$ ) calculated for all compositions cured after 7, 14 and 28 days are presented in Fig. 16, indicating the resistance to physical weathering through wet–dry cycling, a typical stressor in tidal

zones.

Results indicate that GP-based samples generally exhibited lower resistance to slaking compared to traditional Portland cement-based concrete. These observations align with those reported by Samantasinghar and Singh (2021), who studied alkali-activated granular soils with a fly ash (FA) to ground granulated blast furnace slag (GGBS) ratio of 40:60, where the slake durability index improved with increased geopolymer content (ranging from 5 % to 30 %). This discrepancy was more pronounced in samples cured for 28 days compared to 7 days, suggesting that extended curing did not significantly enhance resistance to wet–dry abrasion for certain mix compositions. RSiA and RA-based mix showed higher particle disintegration after two slaking cycles compared to other mixes and this can likely be attributed to the presence of fractured or edge-located RA block particles, which were prone to disintegration upon immersion.

A modified slake durability test tailored for breakwater armour layers was proposed by Acir and Kılıç (2010). Their methodology involved testing 1:30 scale stone models of various sizes under conditions that prevented contact between the specimens and the drum walls, thereby simulating the behaviour of loosely placed armour units in real-world settings. While this method assumes idealized non-contact conditions not always replicated in the field, it effectively demonstrates the potential of the test for evaluating the durability of outer-layer materials. A key finding of their study was that exposure to

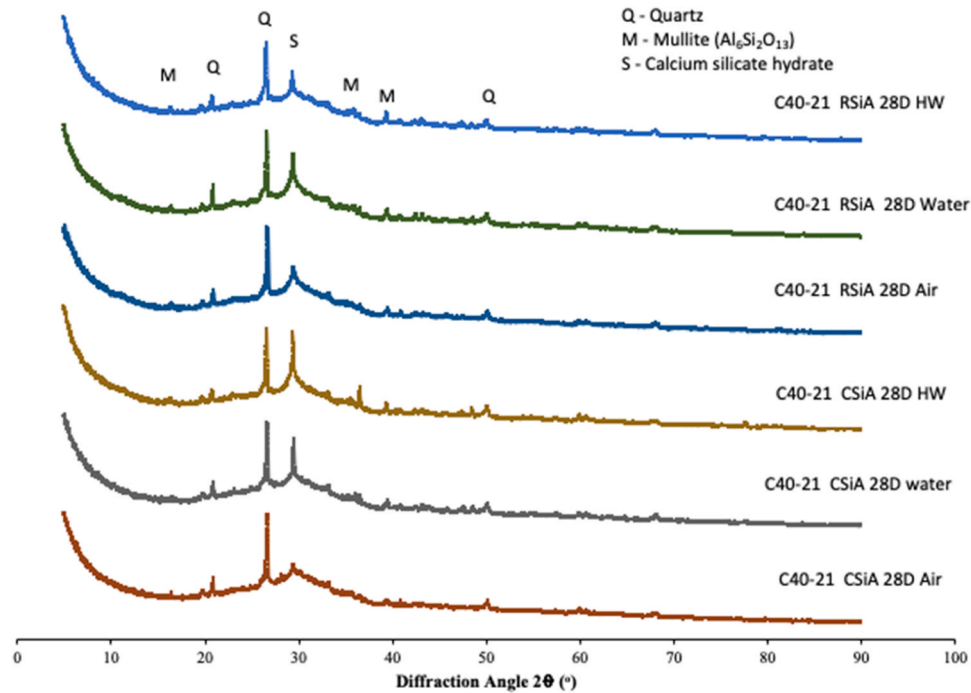


Fig. 12. XRD spectra of pastes made of GGBS, FA, CSiA/RSiA and NaOH cured in air, water 3d hot water and then air.

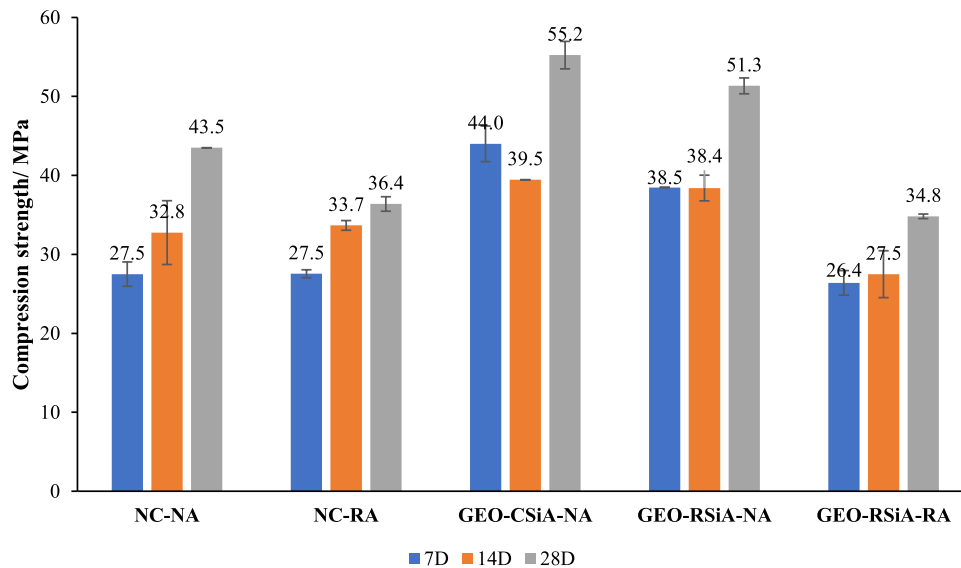


Fig. 13. Compression strength values of the concrete blocks after 7, 14 and 28 days of curing.

saltwater generally enhanced the durability index of larger stones. This is particularly relevant when interpreting the results of the present study, which utilized smaller samples (40–60 g). Larger prototype armour units, typically weighing 1–10 tons, are expected to exhibit reduced edge and corner degradation due to a lower surface area-to-weight ratio, thereby retaining their structural mass more effectively under slaking conditions. In the present investigation, most observed abrasion appeared to originate from the mortar matrix rather than from block disintegration. The tested samples exhibited area-to-weight ratios ranging from 0.006–0.012 cm<sup>2</sup>/g, whereas 1-ton concrete blocks demonstrate much lower ratios, typically between 0.003–0.005 cm<sup>2</sup>/g. When normalized for surface exposure, the rate of weight loss decreased significantly, resulting in a proportionally higher slake durability index, aligning well with the trends reported by [Acir and](#)

[Kılıç \(2010\)](#). As illustrated in [Fig. 17](#), extrapolating Acir and Kılıç's basalt block data (71 g to 361 g), and assuming square geometry for surface calculation, reveals a strong linear relationship between durability index and the inverse area-to-weight ratio. Under saltwater conditions and extended cycling (5000 rotations), extrapolation to a 1-ton equivalent block suggests a slake index approaching 99.87 % at an area-to-weight ratio of 0.00289 cm<sup>2</sup>/g.

Applying this normalization approach to the 28-day cured samples in the current study, namely, the NC-NA and Geo-RSiA-RA revealed notable improvements upon scaling. For NC-NA, the slake index increased from 96.69 % to 99.91 % as the area-to-weight ratio decreased from 1.2 to 0.00326 cm<sup>2</sup>/g. Similarly, the Geo-RSiA-RA mix improved from 88.15 % to 99.67 % over the same range. Although geopolymer-based blocks experienced more rapid corner and edge

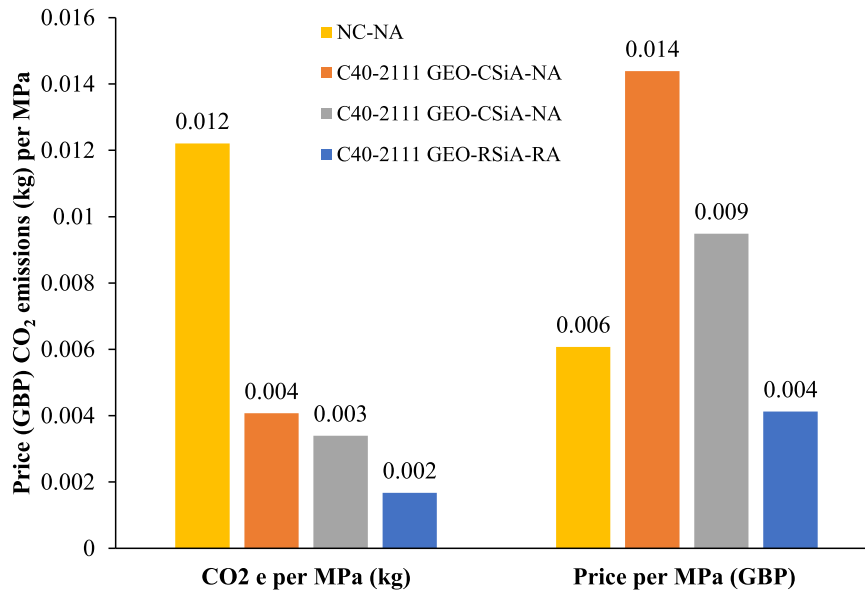


Fig. 14. Calculated price and emissions per 1 MPa of the concrete with CSiA-NA and RSiA-RA.

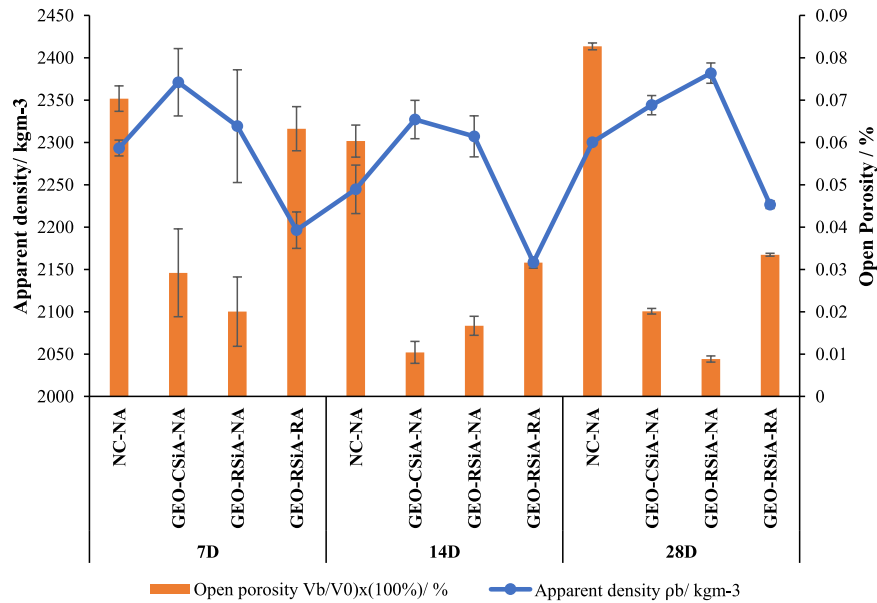


Fig. 15. Open porosity and apparent density of each mix at curing age of 7 days, 14 days and 28 days.

material loss as evident in, the overall reduction in mass at larger scales remains minimal. The images of the samples of GEO-RSiA-RA, before and after the slake test have been illustrated in Fig. 18. These findings reinforce the viability of geopolymer formulations for large-scale coastal applications, provided the scale-dependent behaviour of slake durability is considered in design evaluations.

#### 3.4.3. Chloride migration coefficient

Chloride migration coefficient ( $M_{NS}$ ) of the samples after 7, 14, and 28 days are presented in Fig. 19. Geopolymer blocks showed lower  $M_{NS}$  compared to normal concrete, indicating reduced chloride ingress, enhancing their potential to resist corrosion, a common cause of failure in OPC-based marine structures (Polder et al., 2016). This agrees with open porosity results where concrete had the higher porosity compared to geopolymers. Geopolymer concretes demonstrate inherently low chloride diffusion coefficients ( $10^{-12}$ – $10^{-13}$  m<sup>2</sup>/s) and excellent sulphate resistance due to their aluminosilicate network that lacks portlandite

and C–S–H phases vulnerable to ionic attack (Lee and van Deventer, 2013; Bernal et al., 2014). Field simulations by Nath and Sarker (2015) under 3 % NaCl immersion showed less than 5 % compressive strength loss in fly-ash-based geopolymers after 1 year, compared with over 15 % for OPC controls.

In comparison, OPC-based concrete is susceptible to long-term degradation due to chloride penetration, particularly if not adequately treated or coated (Neville, 2011). Previous studies have shown that geopolymer concretes offer superior resistance to such chemical and physical deterioration (Temuujin et al., 2011; Zhang et al., 2017). Ismail et al. (2013) observed similar results where geopolymer concrete resulted from chloride penetration depths below 10 mm, where normal concrete exhibited a penetration depth of ~25 mm. They have explained that the low penetration depths in geopolymer concrete are attributed to the dense sodium aluminosilicate binding gels (C–N–A–S–H), which hinders chloride migration. Some studies report that introduction of MRAs the geopolymer concrete increased chloride ion penetration depths as



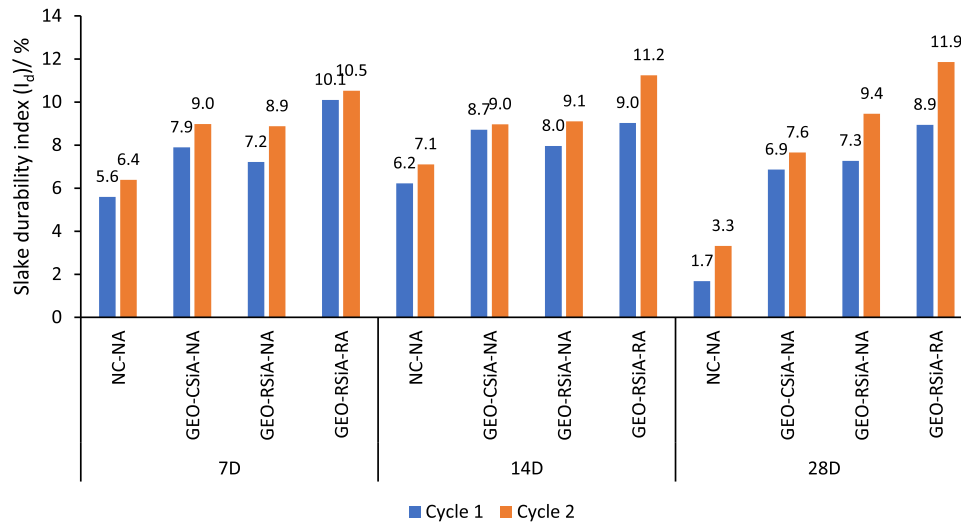


Fig. 16. Slake durability index of mix designs after curing 7, 14 and 28 days.

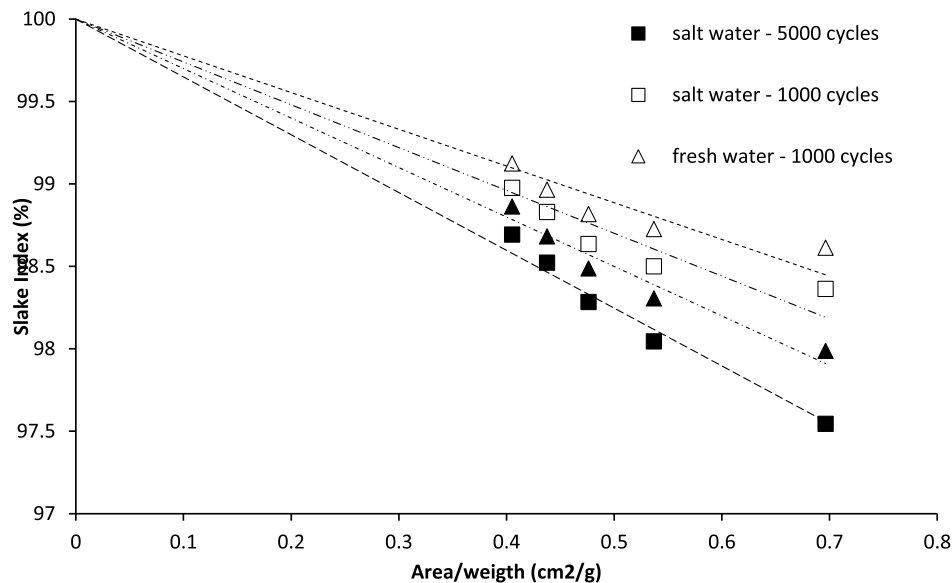


Fig. 17. Slake index prorated by area/weight ratio from [Acr and Kılıç \(2010\)](#) basalt blocks in fresh and salt water.

they adversely affect the interfacial transition zone (ITZ) and introduce micropores and cracks which increase ion permeability ([Nuaklong et al., 2016; Shaikh, 2016; Parthiban et al., 2017; Lyu et al., 2023](#)). The current study used RA which contain ceramic, plastic, metal, clay, glass, concrete or stones but their average consistency was similar to CRA which did not introduce pieces of mortar to the geo-blocks and therefore resistant to permeability of chloride ions together with the geopolymer which mitigates this effect and enhances the bonding of old and new ITZs.

#### 4. Conclusions

This study demonstrates the feasibility and performance of using recycled sodium silicate activator (RSiA) and recycled aggregate (RA) in geopolymer concrete for coastal defence applications. Elemental and FTIR analyses confirmed that RSiA shares comparable chemical characteristics with commercial sodium silicate activators (CSiA), though with higher water content and a lower silicate modulus. Despite this, RSiA-based mixes achieved compressive strengths within the target

range of 20–40 MPa for breakwater structures, with optimized mixes like C40–2111 reaching ~47 MPa under partial hot water curing.

The study found that increasing the GGBS content significantly enhances compressive strength, where FA:GGBS ratio of 40:60 and a Na<sub>2</sub>SiO<sub>3</sub>/NaOH ratio of 2:1 (C40–2111) provides the best balance between mechanical performance, cost, and carbon footprint. Air curing, a more sustainable and scalable method, proved effective in achieving adequate strength (36 MPa for C40–2111) for structural applications.

Durability assessments showed that while geopolymer blocks exhibited slightly lower slake durability than OPC concrete at lab scale, scaling factors suggest minimal material loss in large-scale breakwater units. Additionally, the low chloride migration coefficient and reduced porosity of geopolymer concretes indicate superior resistance to marine corrosion.

Life cycle and cost analyses further highlight the eco-efficiency of geopolymer mixes incorporating recycled materials. The GEO-RSiA-RA mix reduced CO<sub>2</sub> emissions and cost per MPa of strength by up to 45 % and 14 %, respectively, compared to conventional concrete. These outcomes position geopolymer concrete with RSiA and RA as a viable,

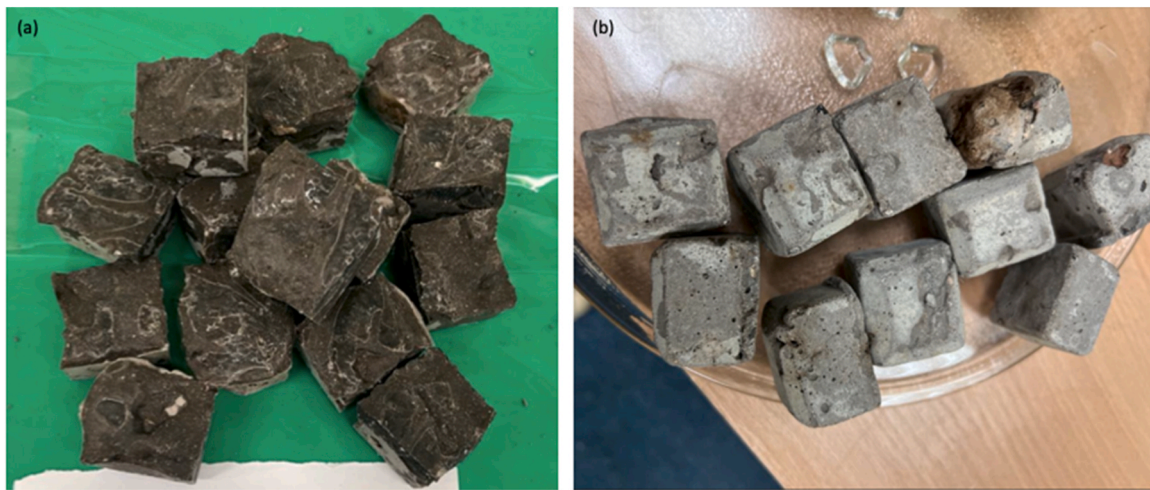


Fig. 18. Geo-RSiA-RA samples (a) before and (b) after slake test.

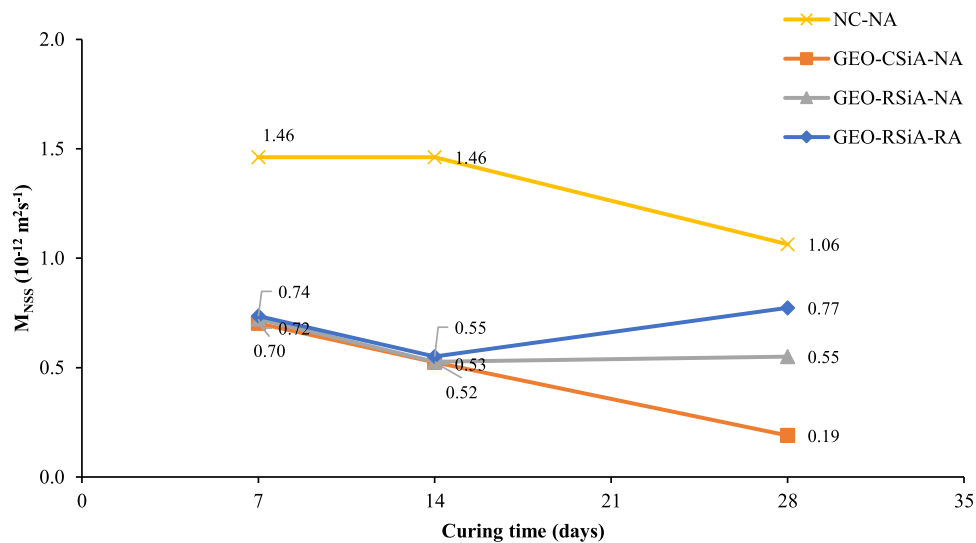


Fig. 19. Chloride migration coefficient of mix designs after curing 7, 14 and 28 days.

sustainable, and high-performing alternative for coastal infrastructure, aligning with global objectives for low-carbon construction and circular resource use.

To further validate its practical application, future research should focus on comprehensive life cycle assessment (LCA) to evaluate environmental benefits across the material's full lifespan. Additionally, long-term durability studies under real marine conditions, including exposure to tidal actions, salinity variations, temperature fluctuations, and freeze-thaw cycles, are essential to assess field performance. The scalability of production techniques for industrial applications must also be explored, along with techno-economic feasibility analyses, to enable large-scale deployment in coastal and offshore structures.

#### CRediT authorship contribution statement

**Wijesekara K.K. D. A.:** Writing – original draft, Investigation, Formal analysis, Data curation. **Monower Sadique:** Writing – review & editing, Writing – original draft, Validation, Supervision, Resources, Project administration, Methodology, Investigation, Funding acquisition, Formal analysis, Data curation. **Gabriela Chronowska Bojczuk:** Formal analysis. **Iacopo Carnacina:** Writing – review & editing, Validation, Supervision, Project administration, Methodology,

Investigation, Formal analysis, Data curation, Conceptualization. **Alis-tair Fielding:** Formal analysis.

#### Declaration of Competing Interest

No conflict of interest associated with this publication.

#### Acknowledgements

The authors of this paper wish to acknowledge the support of the UKRI-Innovate UK under Launchpad advanced manufacturing CR&D Liverpool City Region funding of the research project at Liverpool John Moores University in Collaboration with VIRTUS CONCRETE SOLUTIONS LTD (Grant ID: 10057252).

#### References

- Akduman, Ş., Aktepe, R., Aldemir, A., Özcelikci, E., Alam, B., Sahmaran, M., 2024. 'Opportunities and challenges in constructing a demountable precast building using C&D waste-based geopolymer concrete: a case study in Türkiye'. *J. Clean. Prod.* 434, 139976.
- Aissa, A., Belas, N., Mesbah, H., 2019. Effect of nano-silica addition on the performance of alkali-activated slag/Fly ash pastes and mortars. *Constr. Build. Mater.* 202, 71–83.

- Acir, A., Kılıç, A.M., 2010. A new durability testing method for breakwater concrete armor units: modified slake durability test. *Constr. Build. Mater.* 24 (12), 2416–2423.
- Ali, M.M., Shinde, S.S., Dhawale, S.A., 2017. Guidelines for mix design of Fly ash and GGBS-based alkali activated concrete. *Int. J. Civ. Eng. Technol. (IJCET)* 8 (1), 149–157.
- Bernal, S.A., Provis, J.L., Rose, V., Mejía de Gutiérrez, R., 2012. Effect of silicate modulus and solids content on the performance of alkali-activated slag mortars. *J. Sustain. Cem. Based Mater.* 1 (3), 138–151.
- Bernal, S.A., Provis, J.L., Rose, V., Mejía de Gutiérrez, R., 2014. High-resolution X-ray diffraction and fluorescence microscopy characterization of the steel–geopolymer paste interface. *Cem. Concr. Compos.* 47, 53–62. <https://doi.org/10.1016/j.cemconcomp.2013.11.005>.
- British Standard Institution (2016) BS EN 196-1:2016 – Methods of testing cement – Part 1: Determination of strength. BSI Standards Limited.
- Butler, L., West, J.S., Tighe, S.L., 2011. The effect of recycled concrete aggregate properties on the behaviour of new concrete. *Can. J. Civ. Eng.* 38 (1), 1–13.
- CIRIA (2007) The Rock Manual – The Use of Rock in Hydraulic Engineering. CIRIA C683.
- Crossman, M., Segura-Dominguez, S. and Allsop, W. (2003) Low cost rock structures for beach control and coast protection: Practical design guidance. London: Defra.
- Dadsetan, S., Siad, H., Lachemi, M., Sahmaran, M., 2021a. Evaluation of the tridymite formation as a technique for enhancing geopolymer binders based on glass waste. *J. Clean. Prod.* 278, 123983.
- Dadsetan, S., Siad, H., Lachemi, M., Sahmaran, M., 2021b. Extensive evaluation on the effect of glass powder on the rheology, strength, and microstructure of metakaolin-based geopolymer binders. *Constr. Build. Mater.* 268, 121168.
- Dadsetan, S., Ramezani-pour, A.A., Pilvar, A., 2022. Waste glass-derived silicate activators for sustainable geopolymer concrete: performance evaluation and microstructural analysis. *J. Sustain. Cem. Based Mater.* 11 (4), 215–230.
- Davidovits, J., 1994. Geopolymer cement to minimize carbon-dioxide greenhouse-warming. *Ceram. Trans.* 37, 165–182.
- Davidovits, J. (2020) Geopolymer Chemistry and Applications. 5th edn. Institut Géopolymère.
- Dineshkumar, G., Santhi, A.S., Thenmozhi, R., 2020. Effect of GGBS and activator combinations on mechanical and durability properties of geopolymer concrete. *Mater. Today. Proc.* 33, 499–505. <https://doi.org/10.1016/j.matpr.2020.04.342>.
- Duxson, P., Provis, J.L., 2008. Designing precursors for geopolymer cements. *J. Am. Ceram. Soc.* 91 (12), 3864–3869.
- EIA, U.S. Energy (2023) Annual Greenhouse Gas Emissions Report 2023. U.S. Energy Information Administration.
- EMBER China (2023) Electricity Data and Greenhouse Gas Emissions Report 2023. Ember.
- Environment Agency (2007) Unit Cost Database (2007 Edition). UK Environment Agency.
- European Commission (2007) Best Available Techniques (BAT) Reference Document for the Manufacture of Glass.
- European Environment Agency (2023) Greenhouse Gas Emissions Intensity in the EU-27 Report 2023.
- Federação dos Vidros de Embalagem da Europa (2014) Glass Recycling Achievements and Targets in the UK and EU.
- Fisher, K. and Werge, M. (2009) Waste Management and Recycling in the European Union. European Environment Agency Report.
- Foletto, E.L., et al., 2006. 'Synthesis of sodium silicate from rice husk ash and its application in silica gel production'. *Mater. Res.* 9 (3), 335–339.
- Gao, X., Yu, Q.L., Lazaro, A., Brouwers, H.J.H., 2017. Investigation on a Green olivine nano-silica source based activator in alkali activated slag-Fly ash blends: reaction kinetics, gel structure and carbon footprint'. *Cem. Concr. Res.* 100, 129–139.
- Gaurav, J., Modhera, C., Patel, D., 2024. 'Proposed mixture design method for high-strength geopolymer concrete'. *Acids Mater. J.* 121 (1), 67–78.
- Gholampour, A., Raza, W., Ozbakkaloglu, T., 2023. Utilization of recycled aggregate in geopolymer concrete: a review. *J. Mater. Civ. Eng.* 35 (4), 06023001.
- Gitto, A., Sorelli, L., Tagnit-Hamou, A., Al-Majidi, M.H., 2023. Durability of geopolymer and alkali-activated materials in marine environments: a review. *Cem. Concr. Res.* 164, 107043. <https://doi.org/10.1016/j.cemconres.2022.107043>.
- Hamed, Y.R., Keshta, M.M., Elshikh, M.M.Y., Elshami, A.A., Matthana, M.H.S., Youssef, O., 2025. Performance of sustainable geopolymer concrete made of different alkaline activators. *Infrastructures* 10 (2), 41.
- Habert, G., d'Espinose de Lacaillerie, J.B., Roussel, N., 2011. An environmental evaluation of geopolymer based concrete production: reviewing current research trends. *J. Clean. Prod.* 19 (11), 1229–1238.
- ICE. (2012). ICE Manual of Geotechnical Engineering. Institution of Civil Engineers.
- Imtiaz, L., Kashif-ur-Rehman, S., Alaloul, W.S., Nazir, K., Javed, M.F., Aslam, F., Musarat, M.A., 2021. Life cycle impact assessment of recycled aggregate concrete, geopolymer concrete, and recycled Aggregate-Based geopolymer concrete. *Sustainability* 13 (24), 13515. <https://doi.org/10.3390/su132413515>.
- Ismail, I., Bernal, S.A., Provis, J.L., San Nicolas, R., Hamdan, S., van Deventer, J.S.J., 2013. Modification of phase evolution in alkali-activated blast furnace slag by the incorporation of Fly ash. *Cem. Concr. Compos.* 45, 125–135.
- Kanagaraj, A., Santhanam, M., Mathews, M.S., 2024. Performance assessment of geopolymer concrete under various curing regimes. *Cem. Concr. Compos.* 125, 104668.
- Kathirvel, P., Kaliyaperumal, L., 2016. Mechanical properties of concrete containing recycled aggregate. *Int. J. ChemTech Res.* 9 (1), 146–153.
- King, D.M., Cooper, N.J., Morfett, J.C., Pope, D.J., 2000. Application of offshore breakwaters to the UK: a case study at elmer Beach'. *J. Coast. Res.* 16 (1), 172–183.
- Koushkbaghi, M., Ghanbari, A., Molaei Raisi, S., Samali, B., 2019. The effect of sodium silicate to sodium hydroxide ratios on the durability of Fly ash-based geopolymer concrete. *Constr. Build. Mater.* 222, 796–805. <https://doi.org/10.1016/j.conbuildmat.2019.06.212>.
- Law, D.W., Adam, A.A., Molyneux, T.K.C., Patnaikuni, I., Wardhono, A., 2015. Long term durability properties of class f Fly ash geopolymer concrete. *Mater. Struct.* 48 (3), 721–731.
- Lee, W.H., van Deventer, J.S.J., 2013. Effects of temperature and ionic environment on the strength of Fly ash-based geopolymer concrete. *Cem. Concr. Res.* 42 (2), 314–320.
- Lyu, Y., Liu, J., Wang, S., Yang, Y., 2023. Effects of recycled aggregate content on the performance of geopolymer concrete. *J. Clean. Prod.* 389, 136137.
- Matsumoto, K., Kawai, K., Nakamura, S., 2021. Optimized design of Fly ash-slag blended geopolymer concrete for enhanced durability and mechanical properties. *J. Clean. Prod.* 320, 128906.
- Muis, S., et al., 2020. Future coastal flood risks due to climate change. *Nat. Commun.* 11 (1), 1–12.
- Nath, P., Sarker, P.K., 2017. 'Chloride penetration resistance of concrete containing brick aggregate and supplementary cementitious materials exposed to marine environment'. *Constr. Build. Mater.* 138, 195–204.
- Neville, A.M. (2011). Properties of Concrete. Pearson Education.
- Nuaklong, P., Sata, V., Chindaprasit, P., 2016. Properties of metakaolin-high calcium Fly ash geopolymer concrete containing recycled aggregate from crushed concrete specimens. *Constr. Build. Mater.* 112, 403–410.
- Ostovari, Y., Teymouri, M., Aslani, F., 2020. Durability performance of geopolymer concrete in marine environments: a review'. *Constr. Build. Mater.* 252, 119097.
- Palomo, A., et al., 1999. Alkali-Activated Fly ashes: a cement for the future'. *Cem. Concr. Res.* 29 (8), 1323–1329.
- Parthiban, K., Mohan, A., 2017. Effect of recycled coarse aggregate on fresh and hardened properties of concrete. *Mater. Today. Proc.* 4 (8), 8865–8871.
- Parthiban, K., Saravana Raja Mohan, K., Gobinath, R., 2017. Strength and durability properties of geopolymer concrete made with Ground Granulated Blast-furnace Slag and Black Rice Husk Ash. *KSCE J. Civ. Eng.* 21 (6), 2343–2351.
- Piccinalli, A., Ferone, C., Colangelo, F., 2022. Recycled concrete aggregates for geopolymer concrete: engineering performance and environmental impact. *Materials* 15 (8), 2754.
- Poornima, R., Suguna, K., Bharathi, K.S., 2021. Mechanical and durability performance of alkali-activated Fly ash–GGBS composite concrete under different curing regimes. *Constr. Build. Mater.* 281, 122592.
- Provis, J.L. and Van Deventer, J.S.J. (2013) Alkali Activated Materials: State-of-the-Art Report, RILEM TC 224-AAM. Springer.
- Puertas, F., Torres-Carrasco, M., 2014. Use of glass waste as an activator in the preparation of alkali-activated slag. Mechanical strength and paste characterisation. *Cem. Concr. Res.* 57, 95–104.
- Rashidian-Dezfouli, H., Behfarnia, K., Shojae, S., 2018. Partial replacement of sodium silicate with waste glass in geopolymer concrete: mechanical and durability properties. *Constr. Build. Mater.* 191, 386–399.
- Rodríguez, E.D., Bernal, S.A., Provis, J.L., Payá, J., Monzó, J., 2013. Effect of nanosilica-based activators on the performance of an alkali-activated Fly ash binder. *Cem. Concr. Compos.* 35 (1), 1–11.
- Ryu, G.S., Lee, Y.B., Koh, K.T., Chung, Y.S., 2013. The mechanical properties of Fly ash-based geopolymer concrete with alkaline activators. *Constr. Build. Mater.* 47, 409–418.
- Samantasinghar, S., Singh, S.P., 2021. Geopolymer stabilization of granular soils using Fly ash and GGBS: strength, durability, and microstructural characteristics. *Constr. Build. Mater.* 267, 121032.
- Shaikh, F.U.A., 2016. Mechanical and durability properties of fly ash geopolymer concrete containing recycled coarse aggregates. *Int. J. Sustain. Built Env.* 5 (2), 277–287. <https://doi.org/10.1016/j.ijsbe.2016.06.003>.
- Shaikh, F.U.A., Haque, S., 2019. Durability properties of high-volume Fly ash concrete containing nano-silica. *Mater. Struct.* 52 (2), 36.
- Shoaei, P., Gholampour, A., Ameri, F., 2024. Effect of curing conditions on the mechanical and durability performance of geopolymer concrete. *Constr. Build. Mater.* 342, 129832.
- Singh, B., et al., 2015. Geopolymer concrete: a sustainable alternative to portland cement concrete. *Constr. Build. Mater.* 102, 903–910.
- Temuujin, J., Van Riessen, A., Williams, R., 2011. Influence of calcium compounds on the mechanical properties of Fly ash geopolymer pastes. *J. Hazard. Mater.* 167 (1–3), 82–88. <https://doi.org/10.1016/j.jhazmat.2008.12.121>.
- Tuyan, M., Andıç-Çakır, Ö., Ramyar, K., 2018. Effect of alkali activator concentration and curing conditions on the strength and microstructure of Fly ash-slag based geopolymer concrete. *Constr. Build. Mater.* 180, 8–19.
- U.S. Army Corps of Engineers. (2002). Coastal Engineering Manual (EM 1110-2-1100).
- Vinai, R., Soutsos, M., 2019. Production of sodium silicate powder from waste glass cullet for alkali activation of alternative binders. *Cem. Concr. Res.* 116, 45–56.
- Vinai, R., Soutsos, M.N., Millard, S.G., 2020. Durability performance of alkali activated fly ash–GGBS concrete. *Construction and Building Materials* 246, 118421. <https://doi.org/10.1016/j.conbuildmat.2020.118421>.
- World Bank Group (2018) What a waste 2.0: A global snapshot of solid waste management to 2050. Washington, DC: World Bank.
- Yılmaz, E., Türker, P., Kalkan, E., 2024. High-temperature curing effects on mechanical and microstructural properties of alkali-activated concretes. *Constr. Build. Mater.* 389, 131842.
- Yılmaz, E., Özcan, A., Alzebaree, R., 2024. Microstructural and mechanical characterization of fly ash-based geopolymer pastes activated with different alkaline

- solutions. *Constr. Build. Mater.* 410, 133962. <https://doi.org/10.1016/j.conbuildmatpls.2023.133962>.
- Zhang, Z., Provis, J.L., Reid, A., Wang, H., 2020. Fly ash-based geopolymers: the relationship between composition, pore structure and efflorescence. *Cem. Concr. Res.* 124, 105819.
- Zhang, Z., Provis, J.L., Reid, A., Wang, H., 2022. Fly ash-based geopolymer concrete: the effect of aggregate type on strength and microstructure. *Constr. Build. Mater.* 258, 120578.
- Živica, V., 2006. Effectiveness of new silica fume alkali activator'. *Cem. Concr. Compos.* 28 (1), 21–25.